Electronic Supplementary Material (ESI) for Dalton Transactions.

Supporting Information

Relativistic DFT and Experimental Studies of Mono- and Bis-Actinyl Complexes of an Expanded Schiff-Base Polypyrrole Macrocycle

Xiu-Jun Zheng,[a] Nicola L. Bell,[c] Charlotte J. Stevens,[c] Yu-Xi Zhong,[a] Georg Schreckenbach,[b] Polly L. Arnold,*[c] Jason B. Love*[c] and Qing-Jiang Pan*[a]

[a] Key Laboratory of Functional Inorganic Material Chemistry of Education Ministry, School of Chemistry and Materials Science, Heilongjiang University, Harbin 150080, China

[b] Department of Chemistry, University of Manitoba, Winnipeg, MB, Canada, R3T 2N2

[c] EaStCHEM School of Chemistry, University of Edinburgh, Edinburgh, UK, EH9 3FJ

*Corresponding authors:

panqjitc@163.com (QJ Pan); jason.love@ed.ac.uk (JB Love); polly.arnold@ed.ac.uk (PL Arnold)

Computational Details

In this study, mononuclear M-**pyAn^{m}** and binuclear B-**pyAn^{m}** (An = U, Np and Pu; m = VI and V) of the **L** macrocycle contain 118 and 130 atoms, respectively. More atoms are contained in the **L′** complexes, M-**pyU^{VI}L′** (130), B-**pyU^{VI}L′** (142) and M-**THFU^{VI}L′** (132). Among complexes of the L ligand, M-**pyU^{VI}** and B-**pyPu^{V}** have the least and largest numbers of electrons, corresponding to 572 and 726 electrons, respectively. The basis sets are as follows: Pu/Np/U (34*s*33*p*24*d*18*f*6*g*)/(10*s*9*p*7*d*4*f*1*g*), O (10*s*7*p*3*d*)/(3*s*2*p*1*d*), N (10*s*7*p*3*d*)/(3*s*2*p*1*d*), C(10*s*7*p*3*d*)/(3*s*2*p*1*d*) and H(6*s*2*p*)/(2*s*1*p*). Thus, 1324 orbital basis functions with 3656 auxiliary basis functions were used for M-**pyU^{VI}**, while 1560 orbital functions with 4612 auxiliary functions were employed for B-**pyPu^{V}**.

General Experimental Details

All manipulations were carried out using standard Schlenk line or glovebox techniques under an atmosphere of dinitrogen unless otherwise stated. Pyridine and benzene were distilled from potassium under dinitrogen in a solvent still prior to use. Hexane, diethyl ether, toluene and THF were degassed by sparging with dinitrogen and dried by passing through a column of activated sieves in Vacuum Atmospheres solvent towers. Solvents were stored over activated 4 Å molecular sieves. Deuterated solvents (d_5-pyridine and C_6D_6) were boiled over potassium, vacuum-transferred and freeze-pump-thaw degassed three times prior to use.

H_4L',[1] [n-Bu_4N][BPh_4],[2] [$\{U(OAr)\}_2$(*endo*-BH_4K)(L′)$(THF)_2$] [3] [$(THF)_2(UO_2)(N(SiMe_3)_2)_2$], and [$(py)_2(UO_2)(N(SiMe_3)_2)_2$][4] were synthesised according to modified literature procedures. All other reagents were purchased and used without further purification.

^1H NMR were recorded on either a Bruker AVA400 spectrometer operating at 399.90 or on a Bruker AVA500 operating at 500.12 MHz. $^{13}C\{^1H\}$ NMR spectra were recorded on a Bruker AVA500 operating at 125.76 MHz. Chemical shifts are reported in parts per million and referenced to residual proton resonances calibrated against external TMS ($\delta = 0$ ppm). All spectra were recorded at 298 K unless otherwise stated. Elemental analyses were carried out by Mr Stephen Boyer at London Metropolitan University and by Analytische Laboratorien, Lindlar, Germany.

Cyclic voltammograms were obtained using an Autolab 302 potentiostat and the data processed using GPES Manager version 4.9. Experiments were undertaken in a glove box using a 15 mL glass vial as the cell. The working electrode consisted of a glassy carbon electrode, the counter electrode a platinum mesh and the reference electrode silver wire. The solution employed was ca. 1.0 mM of the compound and 0.1 M [Bu_4N][BPh_4] with scan rates 100–500 mVs^{-1}. All potentials were referenced internally to $CoCp^*_2$ then calibrated against $[Cp_2Fe]^{0/+}$ ($Fc/Fc^+ = 0$ V).

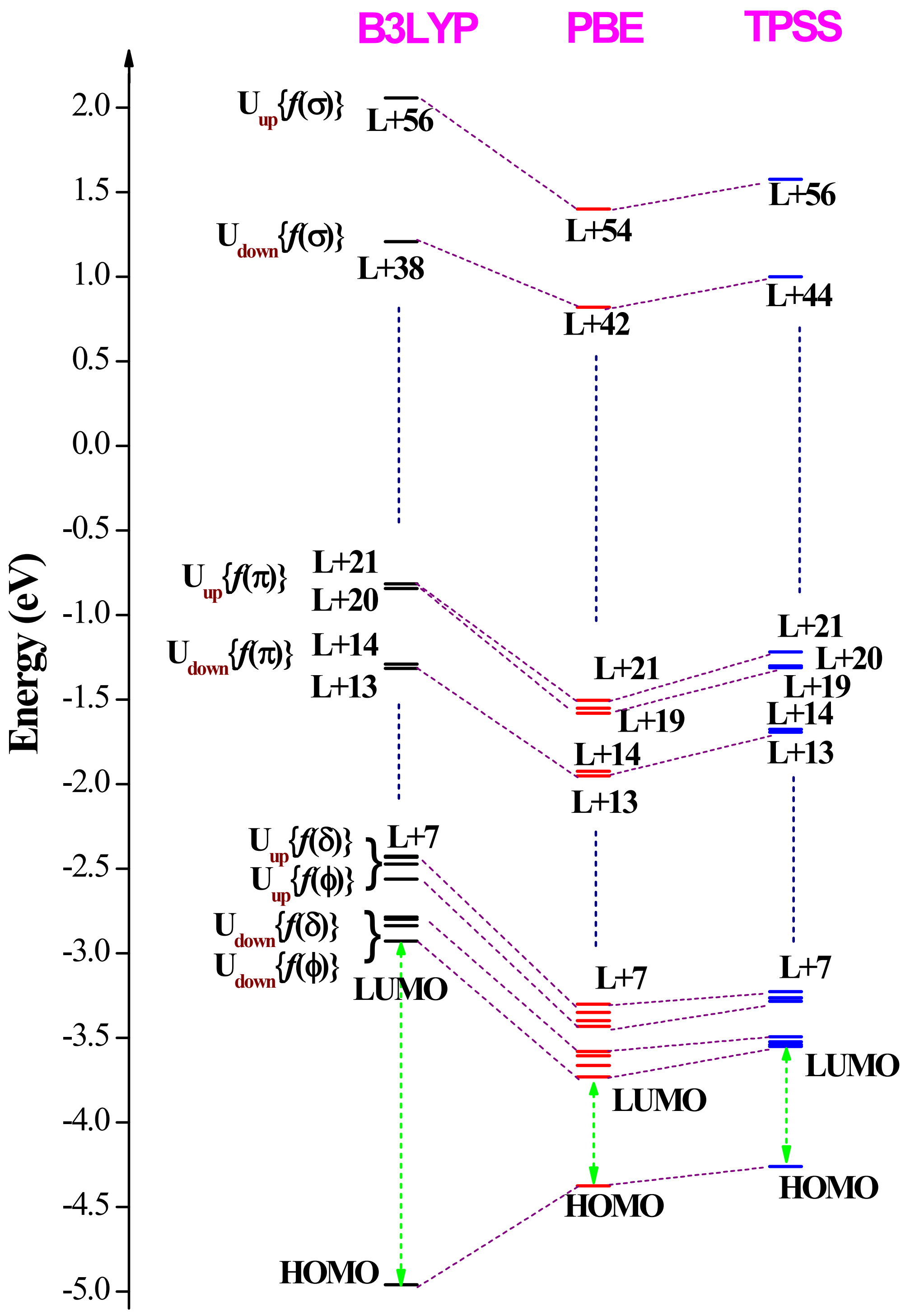

Figure S1. Energetic levels and character of HOMO and unfilled U(*f*) orbitals of B-**pyU**^{VI} calculated with various functionals in the ADF code.

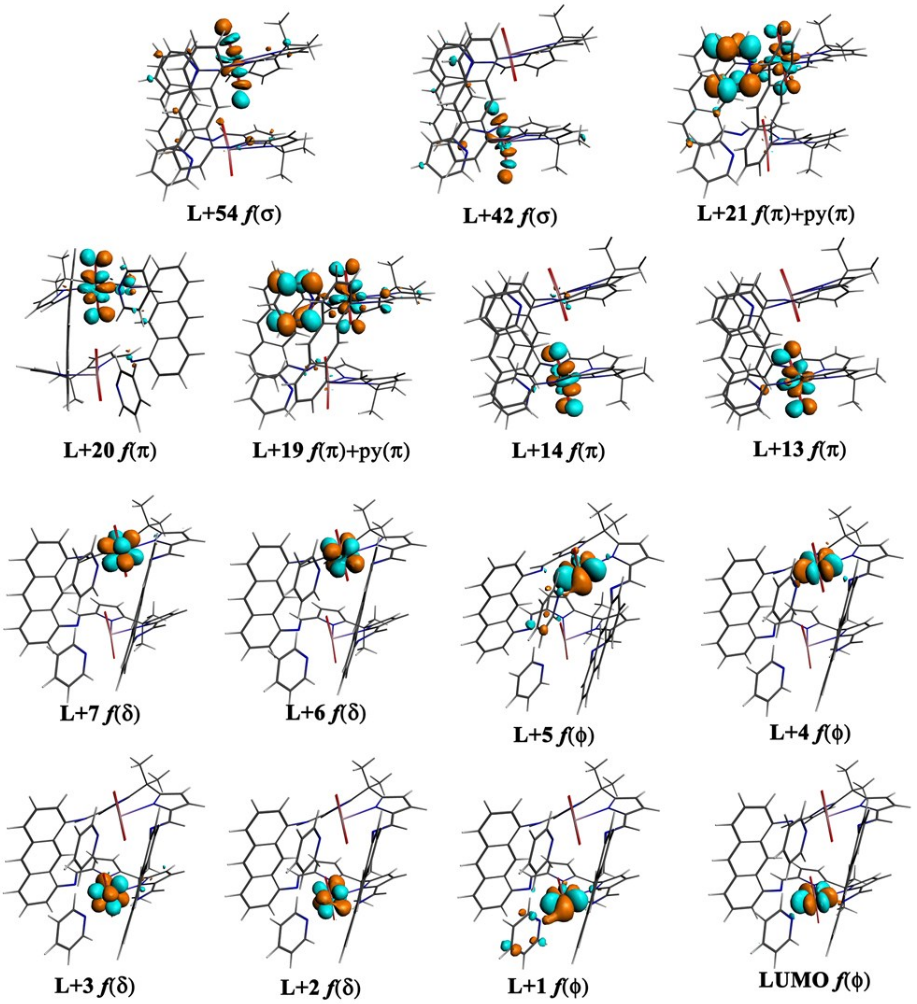

L+54 ***f***(σ) **L+42** ***f***(σ) **L+21** ***f***(π)+py(π)

L+20 ***f***(π) **L+19** ***f***(π)+py(π) **L+14** ***f***(π) **L+13** ***f***(π)

L+7 ***f***(δ) **L+6** ***f***(δ) **L+5** ***f***(ϕ) **L+4** ***f***(ϕ)

L+3 ***f***(δ) **L+2** ***f***(δ) **L+1** ***f***(ϕ) **LUMO** ***f***(ϕ)

Figure S2. Diagrams of unfilled U(*f*) orbitals of B-**pyU**$^{\mathbf{VI}}$ calculated at the ADF: PBE/B-II/ZORA/gas level.

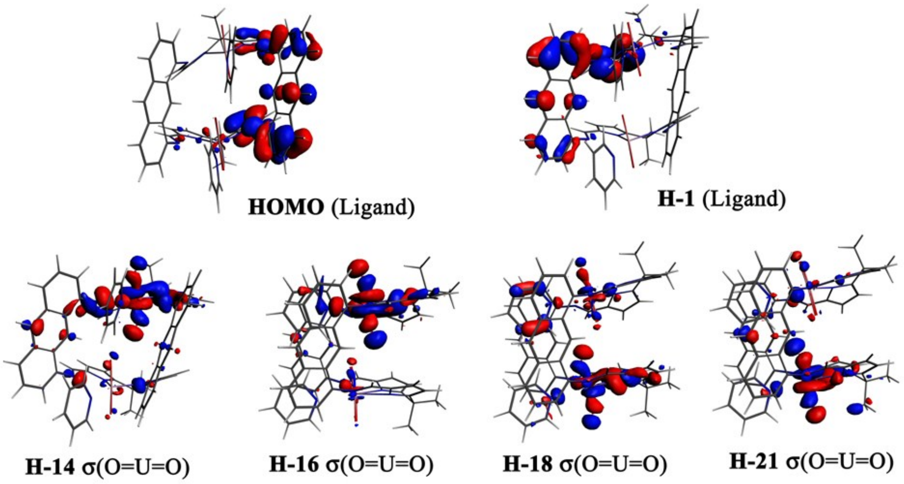

HOMO (Ligand) **H-1** (Ligand)

H-14 σ(O=U=O) **H-16** σ(O=U=O) **H-18** σ(O=U=O) **H-21** σ(O=U=O)

Figure S3. Diagrams of partial occupied orbitals of B-**pyU**$^{\mathbf{VI}}$ calculated at the ADF: PBE/B-II/ZORA/gas level.

Supplementary crystallographic data

CCDC codes for the X-ray structures 1430531-1430533

X-ray crystallographic data were collected at 170 K on an Oxford Diffraction Excalibur diffractometer using graphite monochromated Mo-Kα radiation equipped with an Eos CCD detector Structures were solved using SIR-92 and refined using a full-matrix least square refinement on $|F|^2$ using SHELXL-97.[5] All programs were used within the WinGx suite.[6] All non-hydrogen atoms refined with anisotropic displacement parameters and H-parameters were constrained to parent atoms and refined using a riding model unless otherwise stated.

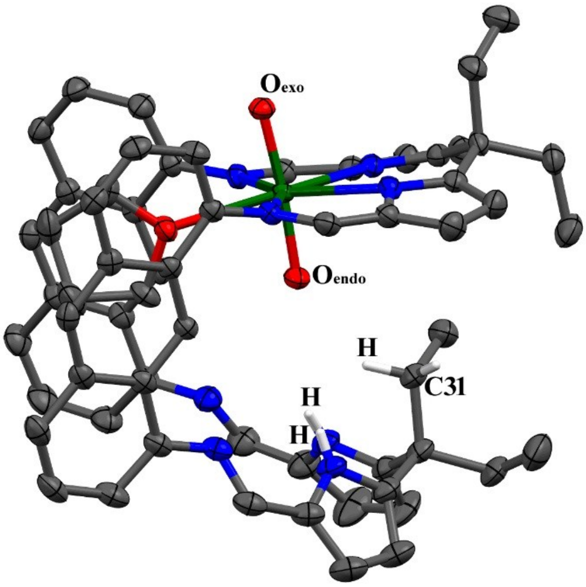

Figure S4. Solid state structure of M-**THFU^{VI}L′**. For clarity, all hydrogens except the pyrrolic NH and those on C31 are omitted (displacement ellipsoids are drawn at 50% probability). Selected distances and angles are shown in Table S2.

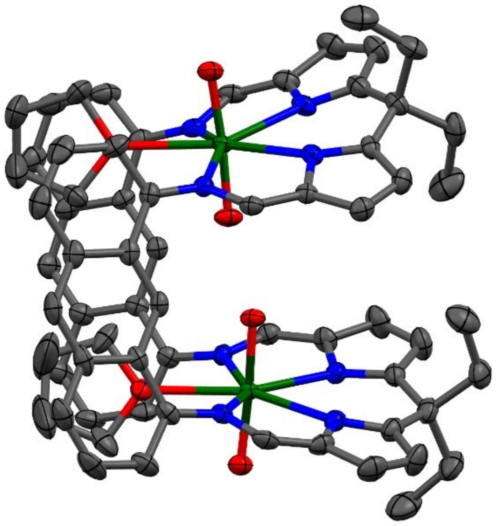

Figure S5. Solid state structure of B-**THFU$^{\mathbf{VI}}$L′**. For clarity, all hydrogens are omitted (displacement ellipsoids are drawn at 50% probability). Selected distances (in Å) and angles (°): U-N_4 plane (0.177 and 0.091), U-O_{exo} (1.772(3) and 1.774(3)), U-O_{endo} (1.754(3) and 1.762(3)), average U-O_{THF} (2.464), average U-$N_{pyrrolide}$ (2.432), average U-N_{imino} (2.563); O-U-O (175.6 and 176.4).

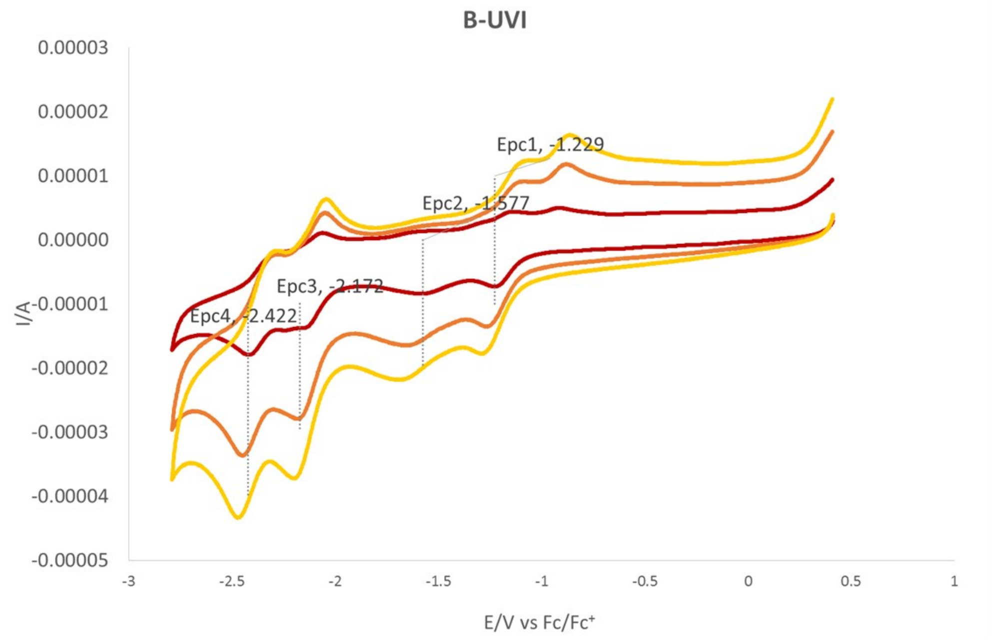

Figure S6. Cyclic Voltammogram of B-**pyU^{VI}L′** under N_2 recorded at 100 mV (red trace), 300 mV (orange trace) and 500 mV (yellow trace) in the range -0.4 V to -2.8 V. Conditions: 0.5 mM of B-**pyU^{VI}L′** in dried and distilled THF, 0.1 M [n-Bu_4N][BPh_4] vs. Fc/Fc^+ (referenced internally to $CoCp^*_2$ then externally to Fc/Fc^+.[7]). Reference electrode: Silver wire, counter electrode: platinum mesh, working electrode: glassy carbon.

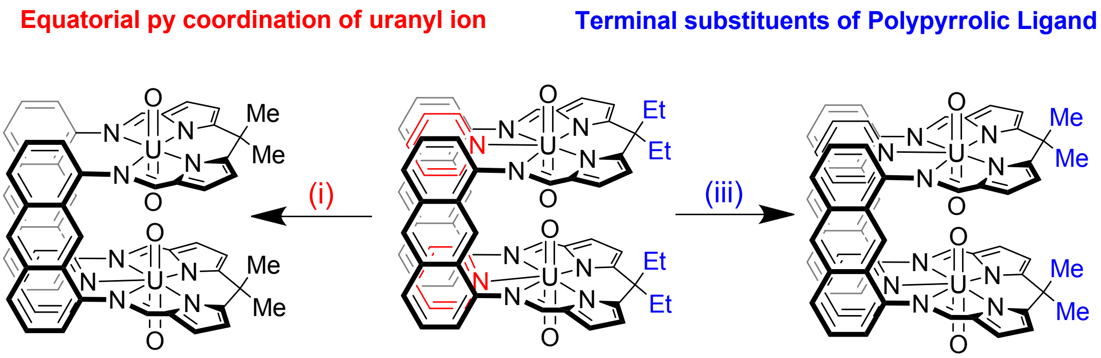

Calculated complex
B-U^{VI}

Experimental complex
B-pyU^{VI}L'

Calculated complex
B-pyU^{VI}

Chart S1. The difference between calculated **B-U^{VI}**/**B-pyU^{VI}** and experimental B-**pyU^{VI}L′.**

Table S1. Calculated (Cal.) and experimentally-synthesized (Expt.) complexes, where L and L′ stand for the methyl and ethyl functionalized ligands, respectively.

		Complexes	Abbreviation
pyridine-solvated complexes	Cal.	Binuclear $[(\mathbf{py})_2(\mathbf{An}^{\mathbf{VI}}O_2)_2(L)]$	B-$\mathbf{pyAn}^{\mathbf{VI}}$ (An = U, Np and Pu)
	Cal.	Binuclear $[(\mathbf{py})_2(\mathbf{An}^{\mathbf{V}}O_2)_2(L)]^{2-}$	B-$\mathbf{pyAn}^{\mathbf{V}}$ (An = U, Np and Pu)
	Cal.	Mononuclear $[(\mathbf{py})(\mathbf{An}^{\mathbf{VI}}O_2)(H_2L)]$	M-$\mathbf{pyAn}^{\mathbf{VI}}$ (An = U, Np and Pu)
	Cal.	Mononuclear $[(\mathbf{py})(\mathbf{An}^{\mathbf{V}}O_2)(H_2L)]^{-}$	M-$\mathbf{pyAn}^{\mathbf{V}}$ (An = U, Np and Pu)
	Cal.	Binuclear $[(\mathbf{py})_2(\mathbf{U}^{\mathbf{VI}}O_2)_2(L')]$	B-$\mathbf{pyU}^{\mathbf{VI}}\mathbf{L'}$
	Cal.	Mononuclear $[(\mathbf{py})(\mathbf{U}^{\mathbf{VI}}O_2)(H_2L')]$	M-$\mathbf{pyU}^{\mathbf{VI}}\mathbf{L'}$
pyridine-free complexes	Cal.	Binuclear $[(\mathbf{An}^{\mathbf{VI}}O_2)_2(L)]$	B-$\mathbf{An}^{\mathbf{VI}}$ (An = U, Np and Pu)
	Cal.	Binuclear $[(\mathbf{An}^{\mathbf{V}}O_2)_2(L)]^{2-}$	B-$\mathbf{An}^{\mathbf{V}}$ (An = U, Np and Pu)
	Cal.	Mononuclear $[(\mathbf{An}^{\mathbf{VI}}O_2)(H_2L)]$	M-$\mathbf{An}^{\mathbf{VI}}$ (An = U, Np and Pu)
	Cal.	Mononuclear $[(\mathbf{An}^{\mathbf{V}}O_2)(H_2L)]^{-}$	M-$\mathbf{An}^{\mathbf{V}}$ (An = U, Np and Pu)
Mixed-valent complex	Cal.	Binuclear $[(\mathbf{py})_2(\mathbf{U}^{\mathbf{VI}}O_2)(\mathbf{U}^{\mathbf{V}}O_2)(L)]^{-}$	B-$\mathbf{pyU}^{\mathbf{VI\text{-}V}}$
py/THF-solvated complexes	Expt.	Binuclear $[(\mathbf{sol})_2(\mathbf{U}^{\mathbf{VI}}O_2)_2(L')]$	B-$\mathbf{solU}^{\mathbf{VI}}\mathbf{L'}$ (sol = py and THF)
	Expt.	Mononuclear $[(\mathbf{sol})(\mathbf{U}^{\mathbf{VI}}O_2)(H_2L')]$	M-$\mathbf{solU}^{\mathbf{VI}}\mathbf{L'}$ (sol = py and THF)
THF-solvated complexes	Cal.	Mononuclear $[(\mathbf{THF})(\mathbf{U}^{\mathbf{VI}}O_2)(H_2L')]$	M-$\mathbf{THFU}^{\mathbf{VI}}\mathbf{L'}$
	Cal.	Mononuclear $[(\mathbf{THF})(\mathbf{U}^{\mathbf{VI}}O_2)(H_2L)]$	M-$\mathbf{THFU}^{\mathbf{VI}}$
	Cal.	Mononuclear $[(\mathbf{THF})(\mathbf{U}^{\mathbf{V}}O_2)(H_2L)]^{-}$	M-$\mathbf{THFU}^{\mathbf{V}}$

Table S2. Optimized and experimental geometry parameters of the mononuclear uranyl complexes equatorially solvated by THF and pyridine ligands, and calculated bond orders are shown in parentheses. (Bond lengths in Å and angles in degree)

	M-**THFU**$^{\mathrm{VI}}$	M-**THFU**$^{\mathrm{VI}}$**L′**	M-**THFU**$^{\mathrm{VI}}$**L′**	M-**THFU**$^{\mathrm{V}}$	M-**pyU**$^{\mathrm{VI}}$	M-**pyU**$^{\mathrm{VI}}$**L′**	M-**pyU**$^{\mathrm{VI}}$**L′**
	Cal.	Cal.	Expt. [a]	Cal.	Cal.	Cal.	Expt. [a]
An-O_{exo}	1.806 (2.39)	1.806 (2.39)	1.776(3)	1.829 (2.38)	1.807 (2.38)	1.808 (2.38)	1.768(2)
An-O_{endo}	1.815 (2.36)	1.815 (2.36)	1.773(3)	1.838 (2.34)	1.818 (2.34)	1.817 (2.35)	1.780(2)
An-N_{py}/O_{THF}	2.486 (0.41)	2.489 (0.41)	2.472(2)	2.544 (0.34)	2.618 (0.37)	2.613 (0.37)	2.565(3)
$O_{endo}\cdots H_1$ (N)	3.206	3.672	3.947	3.203	3.222	3.216	3.989
$O_{endo}\cdots H_2$ (N)	3.188	3.009	3.198	3.169	3.028	3.265	2.802
$O_{endo}\cdots H_3$ (C)	2.489	2.600	2.560	2.382	2.463	2.552	2.654
N-H_1	1.020	1.020	0.76(5) [b]	1.021	1.020	1.020	0.859 [b]
N-H_2	1.020	1.021	0.72(5) [b]	1.021	1.021	1.020	0.861 [b]
C-H_3	1.102	1.104	0.970 [b]	1.102	1.102	1.104	0.970 [b]
O-An-O	174.4	174.5	175.4	174.2	173.7	173.7	175.1
α [c]	10.5	23.7	22.5	10.1	11.0	19.6	22.2
β [c]	5.4	9.5	12.6	7.6	4.8	5.2	12.9
D [c]	8.110	7.971	7.829	8.338	7.791	7.649	7.189

[a] Experimental complexes M-**solU**$^{\mathrm{VI}}$**L′** (sol = py and THF) were structurally characterized in the present work.

[b] Hydrogens placed not found.

[c] The definitions of bite angle (α), twist angle (β) and normal distance (D) are shown in Chart 3.

Table S3. Optimised geometry parameters of B-**pyU**^{VI} and B-**U**^{VI} in the gas phase and pyridine solution using different theoretical approaches, A1 (Priroda: PBE/B-I/AE/gas), A2 (ADF: PBE/B-II/ZORA/gas), A3 (ADF: PBE/B-II/ZORA/COSMO) and A4 (Gaussian: DFT/B-III/RLC-ECP/gas)^{a}. (Distances in Å and angles in degree)

	B-**U**^{VI}									Expt.
	A1	A2	A3	A4-PBE	A4-BP86	A4-TPSS	A4-M06L	A4-B3LYP	A4-PBE0	
U_1-O_{exo}	1.802	1.799	1.810	1.793	1.797	1.794	1.767	1.774	1.751	1.777(4)
U_2-O_{exo}	1.802	1.799	1.810	1.793	1.797	1.794	1.767	1.774	1.751	1.779(4)
U_1-O_{endo}	1.798	1.794	1.794	1.787	1.788	1.787	1.766	1.760	1.746	1.764(4)
U_2-O_{endo}	1.798	1.794	1.794	1.787	1.788	1.787	1.766	1.760	1.746	1.747(4)
U_1-N_{py1}	—	—	—	—	—	—	—	—	—	2.567(5)
U_2-N_{py2}	—	—	—	—	—	—	—	—	—	2.611(6)
$O_{endo}\cdots O_{endo}$	2.940	2.880	2.886	2.907	2.853	2.913	2.928	2.872	2.855	2.708
$U\cdots U$	5.106	5.175	5.143	5.144	5.433	5.212	4.838	5.789	5.089	5.699
O_{exo}-U_1-O_{endo}	175.6	175.8	176.7	175.6	174.9	175.4	175.0	174.1	176.4	174.0
O_{exo}-U_2-O_{endo}	175.6	175.8	176.7	175.6	175.0	175.4	175.0	174.1	176.4	176.0
α	40.5	34.9	35.9	36.5	33.0	35.8	37.9	36.1	36.1	16.8
β	38.4	36.3	37.1	39.3	32.1	37.6	42.6	28.5	39.1	22.6
θ(f)	172.5	174.7	173.3	170.3	173.4	165.8	169.7	177.7	167.7	177.3
θ(s)	123.5	130.5	129.7	127.6	137.3	129.1	122.6	143.2	129.3	172.9
D	4.262	5.059	4.833	4.339	5.590	4.716	3.687	5.926	4.316	6.819

	B-**pyU**^{VI}									Expt.
	A1	A2	A3	A4-PBE	A4-BP86	A4-TPSS	A4-M06L	A4-B3LYP	A4-PBE0	
U_1-O_{exo}	1.811	1.810	1.816	1.802	1.805	1.803	1.776	1.779	1.761	1.777(4)
U_2-O_{exo}	1.810	1.811	1.818	1.800	1.803	1.801	1.774	1.777	1.759	1.779(4)
U_1-O_{endo}	1.793	1.798	1.796	1.782	1.786	1.783	1.760	1.759	1.742	1.764(4)
U_2-O_{endo}	1.801	1.790	1.789	1.791	1.795	1.790	1.769	1.777	1.748	1.747(4)
U_1-N_{py1}	2.628	2.646	2.610	2.638	2.633	2.631	2.616	2.644	2.606	2.567(5)
U_2-N_{py2}	2.653	2.619	2.578	2.662	2.667	2.660	2.617	2.673	2.628	2.611(6)
$O_{endo}\cdots O_{endo}$	2.786	2.753	2.735	2.820	2.838	2.850	2.706	2.766	2.758	2.708
$U\cdots U$	5.934	5.896	5.922	5.943	5.974	6.007	5.638	5.946	5.866	5.699
O_{exo}-U_1-O_{endo}	170.5	170.3	171.9	174.4	174.4	174.2	173.7	174.7	175.5	174.0
O_{exo}-U_2-O_{endo}	174.3	173.5	174.8	172.1	172.3	172.5	170.8	173.2	173.9	176.0
α	17.0	12.1	13.3	15.0	16.9	16.0	1.5	16.3	15.8	16.8
β	13.2	11.1	11.0	13.4	13.2	13.3	14.3	12.5	14.5	22.6
θ(f)	177.4	177.7	178.0	174.7	174.1	174.7	177.9	175.9	173.2	177.3
θ(s)	174.5	166.2	167.6	176.7	177.2	178.5	169.5	178.2	177.7	172.9
D	7.189	7.546	7.621	7.413	7.488	7.354	6.930	7.597	7.269	6.819

[a] In the approach A4 (Gaussian: DFT/B-III/RLC-ECP/gas), various functionals, Stuttgart relativistic large-core effective core potentials (RLC-ECPs), and basis sets (labeled as B-III) associated with the RLC pseudopotentials were used. The Stuttgart RLC ECP basis sets were obtained from EMSL Basis Set Exchange Library (https://bse.pnl.gov/bse/portal).

Table S4. Optimized geometry parameters and bond orders (in parentheses) for equatorially pyridine-free binuclear actinyl complexes. (Distances in Å and angles in degree)

	B-**U**^{VI}	B-**U**^{V}	B-**Np**^{VI}	B-**Np**^{V}	B-**Pu**^{VI}	B-**Pu**^{V}
An-O$_{exo}$	1.802	1.827	1.797	1.821	1.783	1.816
	(2.39)	(2.38)	(2.36)	(2.36)	(2.35)	(2.34)
An-O$_{endo}$	1.798	1.817	1.792	1.811	1.778	1.800
	(2.38)	(2.37)	(2.35)	(2.35)	(2.34)	(2.34)
O$_{endo}\cdots$O$_{endo}$	2.940	3.116	2.906	3.035	2.935	3.011
An$\cdots$O$_{endo}$	3.931	4.043	3.943	4.001	3.973	4.060
O$_{exo}$-An-O$_{endo}$	175.6	176.1	176.5	176.3	178.3	177.3

Table S5. Optimized geometry parameters and bond orders (in parentheses) for equatorially pyridine-free mononuclear actinyl complexes. (Distances in Å and angles in degree)

	M-**U**^{VI}	M-**U**^{V}	M-**Np**^{VI}	M-**Np**^{V}	M-**Pu**^{VI}	M-**Pu**^{V}
An-O$_{exo}$	1.801	1.830	1.787	1.817	1.785	1.809
	(2.40)	(2.39)	(2.38)	(2.38)	(2.35)	(2.36)
An-O$_{endo}$	1.817	1.853	1.802	1.851	1.801	1.837
	(2.30)	(2.24)	(2.29)	(2.20)	(2.26)	(2.19)
O$_{endo}\cdots$H	2.034	1.946	2.041	1.862	2.093	1.882
	(0.05)	(0.08)	(0.05)	(0.10)		(0.10)
O$_{exo}$-An-O$_{endo}$	176.3	173.6	178.9	176.5	179.6	177.8

Table S6. Experimental details for X-ray crystal structures.

name	M-**pyU$^{\mathrm{VI}}$L′**	M-**THFU$^{\mathrm{VI}}$L′**	B-**THFU$^{\mathrm{VI}}$L′**
Chemical formula	$C_{75}H_{67}N_9O_2U$	$C_{70}H_{74}N_8O_5U$	$C_{66}H_{64}N_8O_6U_2 \cdot 4(C_4H_8O)$
M_r	1364.40	1345.41	1829.72
Crystal system, space group	Monoclinic, $P2_1/n$	Triclinic, $P\bar{1}$	Triclinic, $P\bar{1}$
a, b, c (Å)	22.2921 (4), 11.1308 (2), 24.7662 (5)	12.1947 (2), 13.7113 (2), 22.6712 (3)	14.2852 (2), 16.2683 (3), 17.1398 (3)
α, β, γ (°)	90, 91.639 (2), 90	77.050 (1), 80.069 (1), 71.238 (1)	96.866 (2), 102.010 (1), 91.407 (1)
V (Å^3)	6142.7 (2)	3477.26 (9)	3863.08 (11)
Z	4	2	2
μ (mm^{-1})	2.70	2.44	4.25
Crystal size (mm)	0.57 × 0.24 × 0.04	0.87 × 0.22 × 0.16	0.35x0.17x0.05
$T_{\min}$, $T_{\max}$	0.299, 0.869	0.659, 1.000	0.675, 1.000
No. of measured	87824	15937	63978
independent	14074	15937	15789
and observed [$I > 2\sigma(I)$] reflections	10663	14537	12604
R_{int}	0.061	0.036	0.042
$(\sin \theta/\lambda)_{\max}$ (Å^{-1})	0.649	0.649	0.625
$R[F^2 > 2\sigma(F^2)]$, $wR(F^2)$, S	0.035, 0.078, 1.00	0.029, 0.079, 1.00	0.035, 0.089, 0.93
No. of parameters	775	788	919
No. of restraints	38	61	215
H-atom treatment	riding	riding and placed	riding
$\Delta\rangle_{\max}$, $\Delta\rangle_{\min}$ (e Å^{-3})	1.21, -0.85	1.11, -0.68	1.87, -0.70

Table S7. Correction energy (eV) of spin-orbit coupling (SOC) and multiplet effects for the single-electron reduction reaction of mono- and binuclear uranyl complexes.

Single-electron reaction		ΔE_{SOC}	$\Delta E_{Multiplet}$	ΔE_{tot}
M-**pyU**$^{VI\rightarrow V}$	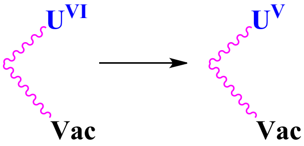	0.31	0.00	0.31
B-**pyU**$^{VI\text{-}VI\rightarrow VI\text{-}V}$	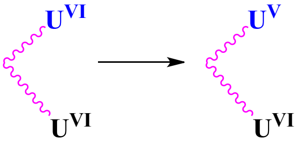	0.31	0.00	0.31
		0.00	0.00	0.00
B-**pyU**$^{VI\text{-}V\rightarrow V\text{-}V}$	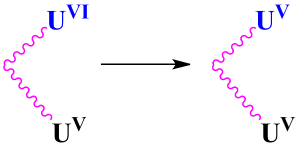	0.31	0.00	0.31
		0.31	*0.78* [a]	***1.09***

[a] The empirical value of the multiplet effect comes from the couple $[Np^{VI}(H_2O)_5]^{2+}/[Np^{V}(H_2O)_5]^{+}$ (Ref. [8]).

References

The full reference of the ADF code:

E. J. Baerends, T. Ziegler, J. Autschbach, D. Bashford, A. Bérces, F. M. Bickelhaupt, C. Bo, P. M. Boerrigter, L. Cavallo, D. P. Chong, L. Deng, R. M. Dickson, D. E. Ellis, M. van Faassen, L. Fan, T. H. Fischer, C. Fonseca Guerra, A. Ghysels, A. Giammona, S. J. A. van Gisbergen, A. W. Götz, J. A. Groeneveld, O. V. Gritsenko, M. Grüning, S. Gusarov, F. E. Harris, P. van den Hoek, C. R. Jacob, H. Jacobsen, L. Jensen, J. W. Kaminski, G. van Kessel, F. Kootstra, A. Kovalenko, M. V. Krykunov, E. van Lenthe, D. A. McCormack, A. Michalak, M. Mitoraj, J. Neugebauer, V. P. Nicu, L. Noodleman, V. P. Osinga, S. Patchkovskii, P. H. T. Philipsen, D. Post, C. C. Pye, W. Ravenek, J. I. Rodríguez, P. Ros, P. R. T. Schipper, G. Schreckenbach, J. S. Seldenthuis, M. Seth, J. G. Snijders, M. Solà, M. Swart, D. Swerhone, G. te Velde, P. Vernooijs, L. Versluis, L. Visscher, O. Visser, F. Wang, T. A. Wesolowski, E. M. van Wezenbeek, G. Wiesenekker, S. K. Wolff, T. K. Woo, A. L. Yakovlev, ADF2010.02 ed., SCM, Theoretical Chemistry, Vrije Universiteit, Amsterdam, The Netherlands, **2010**.

The full reference of the Gaussian code:

M. J. Frisch, G. W. Trucks, H. B. Schlegel, G. E. Scuseria, M. A. Robb, J. R. Cheeseman, G. Scalmani, V. Barone, B. Mennucci, G. A. Petersson, H. Nakatsuji, M. Caricato, X. Li, H. P. Hratchian, A. F. Izmaylov, J. Bloino, G. Zheng, J. L. Sonnenberg, M. Hada, M. Ehara, K. Toyota, R. Fukuda, J. Hasegawa, M. Ishida, T. Nakajima, Y. Honda, O. Kitao, H. Nakai, T. Vreven, J. A. Montgomery, Jr., J. E. Peralta, F. Ogliaro, M. Bearpark, J. J. Heyd, E. Brothers, K. N. Kudin, V. N. Staroverov, R. Kobayashi, J. Normand, K. Raghavachari, A. Rendell, J. C. Burant, S. S. Iyengar, J. Tomasi, M. Cossi, N. Rega, J. M. Millam, M. Klene, J. E. Knox, J. B. Cross, V. Bakken, C. Adamo, J. Jaramillo, R. Gomperts, R. E. Stratmann, O. Yazyev, A. J. Austin, R. P. Cammi, C., J. W. Ochterski, R. L. Martin, K. Morokuma, V. G. Zakrzewski, G. A. Voth, P. Salvador, J. J. Dannenberg, S. Dapprich, A. D. Daniels, O. Farkas, J. B. Foresman, J. V. Ortiz, J. Cioslowski and D. J. Fox, Gaussian, Inc., Wallingford CT, Gaussian 09, Revision D.01 edn., **2009**.

1. E. Askarizadeh, A. M. J. Devoille, D. M. Boghaei, A. M. Z. Slawin and J. B. Love, *Inorg. Chem.*, 2009, **48**, 7491-7500.
2. W. J. Ramsay and J. R. Nitschke, *J. Am. Chem. Soc.*, 2014, **136**, 7038-7043.
3. P. L. Arnold, C. J. Stevens, R. M. Lord, G. S. Nichol and J. B. Love, *In preparation*, 2016.
4. D. M. Barnhart, C. J. Burns, N. N. Sauer and J. G. Watkin, *Inorg. Chem.*, 1995, **34**, 4079-4084.
5. G. Sheldrick, *Acta Crystallogr., Sect. A*, 2008, **64**, 112-122.
6. L. Farrugia, *J. Appl. Crystallogr.*, 1999, **32**, 837-838.
7. J. R. Aranzaes, M.-C. Daniel and D. Astruc, *Can. J. Chem.*, 2006, **84**, 288-299.
8. P. J. Hay, R. L. Martin and G. Schreckenbach, *J. Phys. Chem. A*, 2000, **104**, 6259-6270.